Systematic Investigation of Preparing Biocompatible, Single, and Small ZnS-Capped CdSe Quantum Dots with Amphiphilic Polymers

Robin E. Anderson[†] and Warren C. W. Chan[†,‡,*]

[†]Institute of Biomaterials & Biomedical Engineering, Centre for Biomaterials and Biomolecular Research, and [‡]Department of Materials Science and Engineering, University of Toronto, Toronto, ON, Canada

ABSTRACT The successful transfer of nanoparticles between solvents is critical for many applications. We evaluated the impact of amphiphilic polymer composition on the size, transfer efficiency, and biocompatibility of tri-*n*-octylphosphine oxide/hexadecylamine-stabilized semiconductor ZnS-capped CdSe and CdS-capped $CdTe_xSe_{1-x}$ quantum dots (QDs). We also investigated the adsorption of various proteins onto the surface of these QDs and studied the effect of surface chemistry on non-specific protein binding. The results from these studies will have implications in the design of QDs and other nanoparticles for biological and biomedical applications.

KEYWORDS: quantum dots · semiconductor nanoparticles · amphiphilic polymer · polymer wrapping · protein adsorption

In the last 20 years, we have seen an explosion in research dealing with the synthesis and characterization of nanoparticles.[1–3] Researchers have used unique and interesting reaction conditions to prepare nanoparticles of different sizes, shapes, and compositions.[4–8] Certain reaction conditions restrict the polarity, surface chemistry, and solubility of the nanoparticles. The ability to rapidly and efficiently transfer nanoparticles between solvents is important for many of their applications. Currently, there are three common methods to transfer nanoparticles between organic and aqueous solvents. Perhaps, the simplest method to change the solubility of a nanoparticle is *via* the technique of molecular exchange.[9–11] In this method, an external molecule (*e.g.*, mercaptoacetic acid) is added to a solution of nanoparticle (*e.g.*, quantum dots) in a specific solvent (*e.g.*, chloroform), and this molecule competes for binding sites onto the nanoparticle surface with the original surface ligand (*e.g.*, tri-*n*-octylphosphine oxide, TOPO). Using this example, the polarity and surface chemistry of the nanoparticles are altered when the surface ligand (TOPO) is displaced by the external molecule (*e.g.*, mercaptoacetic acid). The nanoparticles become hydrophilic and contain carboxylic acid groups on the surface for conjugation. However, the dative adsorption of surface ligands is relatively weak, could desorb from the surface, and lead to nanoparticle aggregation. In a second method, the external molecule could be an amphiphilic molecule (*e.g.*, phospholipids), and this molecule could interact with the hydrophobic portion of the surface ligand on the nanoparticle.[12–15] The end result of this modification process is a nanoparticle with a hydrophilic functional group on their surface. In other methods, nanoparticles could be incorporated inside a microsphere (*e.g.*, silica nanoparticles), liposome, or hydrogel for modification of polarity and functionality.[16–18] These final encapsulated structures could be large in comparison to the original size of the nanoparticle. Despite advances in this area of research, much work is still required.

The use of nanoparticles in biomedical applications hinges on the ability to manipulate the surface chemistry. For many biomedical applications, nanoparticles need to be small, biocompatible, monodisperse, and available functional groups for conjugation. Recently, the use of amphiphilic polymers for this purpose has been a major focus. Parak and co-workers[13] and Colvin and co-workers[15] demonstrated the use of poly(maleic anhydride-alt-1-octadecene) to water solubilize magnetic, semiconductor, and metallic nanoparticles. Disappointingly, this particular amphiphilic polymer is no longer commercially available. Other amphilphilic polymers currently under investi-

*Address correspondence to warren.chan@utoronto.ca.

Received for review December 31, 2007 and accepted May 20, 2008.

Published online June 14, 2008.
10.1021/nn700450g CCC: $40.75

gation include block copolymers (*e.g.*, polystyrene-*b*-poly(acrylic acid)),[19] poly(methyl methacrylate)−poly(ethyleneoxide),[20] and amphiphilic hyperbranched polyethylenimine.[21] Other groups have also demonstrated the synthesis of an amphiphilic polymer and demonstrated the wrapping of these polymers to solubilize nanoparticles in aqueous solvents.[14,22,23] However, a thorough characterization of these polymers and a systematic evaluation of the wrapping of the polymers around the nanoparticles were not fully described. Our group and others have had some difficulty in reproducing this coating scheme. In this paper, we aim to synthesize an amphiphilic polymer using commercially available reagents, investigate the effect of polymer composition on the water solubilization of semiconductor nanocrystals, and characterize the non-specific interactions of the polymer-wrapped nanocrystals with proteins. The last aim is important because protein adsorption can affect the use of nanocrystals in biomedical applications or could be important in dictating the toxicity of the nanocrystals.[24–27]

Semiconductor nanocrystals, also known as quantum dots (QDs), have been the subject of intense research in the past 20 years due to their size- and composition-tunable optoelectronic properties. [28–31] A diverse range of applications has been proposed for QDs. Compared to organic fluorophores, QDs could be tuned with narrower emission profiles, broader excitation spectra, are brighter and more resistant to photobleaching.[9,28] These properties are advantageous in many biomedical applications. Despite a growing trend of aqueous-based techniques to synthesize QDs, the best methods to prepare high-quality QDs still lie with either the organometallic or greener method.[7,32–36] In order to use these QDs for biomedical applications, their surfaces must be modified so that they are water-soluble, biocompatible, and maintain the optical properties of the organic-soluble QDs. A number of recent reports have described various methods to address these issues.[14,20,37,38] In biological applications, the most commonly used method for water-solublizing QDs is to wrap their surface with an amphiphilic polymer (method 2 in an earlier discussion). This is due to the QDs' commercial availability.[14,39] The typical amphiphilic polymer consists of a hydrophilic backbone (usually poly(acrylic acid)) modified with long hydrophobic alkyl chains. These hydrophobic groups can then interdigitate with the TOPO and/or HDA ligands on the QD surface, leaving the unmodified portion of the backbone exposed to the environment with the hydrophilic groups (such as carboxylic acids) protruding from the surface of the QDs. In this paper, we aim to systematically develop a procedure to prepare QDs with an amphiphilic polymer coating.

RESULTS AND DISCUSSION

In order to optimize the wrapping of the QDs with the amphiphilic polymer, we initially prepared a wide variety of the amphiphilic polymers. We investigated whether the hydrophobic chain length and the degree of polymer modification affected the transfer of organic-soluble QDs to water.

Amphiphilic Polymer Synthesis and Characterization. A library of amphiphilic polymers was synthesized for this study. See Figure 1a for a schematic of the reaction. Specifically, amine-terminated alkyl molecules such as OA, DDA, HDA, and ODA were mixed with PAA in MPD with DCC. MPD is an aprotic solvent suitable for a DCC conjugation reaction since it has a high boiling point (202 °C) and dissolves PAA, DCC, and the alkylamine. It was used in the original literature reference for this reaction. However, any aprotic solvent with similar characteristics could be used.

A chemical bond between the amine-terminated alkyl molecules with PAA is confirmed by a ninhydrin assay. Ninhydrin reacts with free amines in the sample and forms a colored product. The amount of amine in the sample is determined by measuring the absorbance at 570 nm. Using this method, a decrease in ODA concentration confirms that octadecylamine has been conjugated to PAA. The change in the ODA concentration allows for calculation of the efficiency of that reaction. For example, we performed a ninhydrin assay on the 40% ODA−PAA reaction mixture before any conjugation (ODA + PAA only) to establish a known initial absorbance value for the total amine in the sample prior to conjugation. After the conjugation of ODA to PAA had taken place (and prior to any cleaning steps), a second ninhydrin assay was performed to obtain a final absorbance value. Initial and final concentration values were calculated from the absorbance values using Beer's law and an extinction coefficient of 0.3556 mM^{-1} cm^{-1} (see Figure S1 in Supporting Information). Comparing the initial and final concentration values, the % of alkylamine bonded to the PAA after the reaction was calculated to be 96.7 % for the 40% ODA−PAA reaction. When this ninhydrin assay was repeated for the other ODA polymers, % was determined to be >90% for the different combinations (see Table S1 in Supporting Information). In preparing the polymer, our aim was not to saturate the carboxylic acid functional groups with the amines from the alkylamines since the carboxylic acids were required to solubilized the QDs in aqueous buffer. Our data show that, in this reaction, the reaction efficiency is close to unity. Using stoichiometry of the reactants, we can approximate the number of hydrophobic chains and carboxylic acids on the final polymer.

Another method of confirming the chemical bond between the amine-terminated alkyl molecules with PAA is by FTIR measurements. The FTIR spectrum shows the presence of an amide peak at ~3330 nm for all con-

jugated polymers. Unfortunately, all of the carboxylic acid peaks were obscured by moisture peaks which were not removed even after desiccation for 24 h, so the anticipated decrease in carboxylic acid peak intensity with increased degree of reaction could not be verified.

PAA is not soluble in chloroform; however, all of the modified polymers had some degree of solubility in chloroform. A change in solubility is another indicator of a successful reaction. Generally, as the concentration of hydrophobic side chains with the alkylamine on the PAA increases, so does their solubility in chloroform. Polymers with 20−50% DDA, HDA, and ODA were easily soluble in chloroform. All 10% modified polymers and all OA-modified polymers were only minimally soluble in chloroform. Empirically, solubility in chloroform seems to correlate with the ability of a polymer to efficiently interdigitate with QD surface ligands and solubilize the QD in water.

In past literature, it was stated that MS and ^{1}H NMR were used to confirm the degree of modification, but no data were ever shown.[15,40] In our experience, MALDI mass spectrometry (Applied Biosystems Voyager-DE STR mass spectrometer, Foster City, CA) was not helpful in determining the degree of polymer modification (see Figure S2 in Supporting Information). Since the starting reactant material PAA had an average molecular weight of 1773 ± 1022 g/mol, the resulting modified polymers would also have a dispersity of molecular weights. Also, after modification, some of the polymers do not have a sufficiently high solubility in either water or chloroform, and this resulted in low intensity counts in the mass spectra. The polydispersity of molecular weight and the low intensity counts combined to produce MS did not provide meaningful data. ^{1}H NMR had the same problems that MS had because of the polydispersity of the polymers.

We, therefore, estimated the size of the final polymer using gel electrophoresis. The polymers were run on an agarose gel against a protein panel with a molecular weight range of 2 to 212 kDa (see Figure S3 in Supporting Information). The lowest molecular weight protein in this panel was the B chain protein, which has a molecular weight of 2340 g/mol. When 10−50% ODA−PAA polymers was ran against the protein panel, we observed that 40% ODA−PAA ran approximately the same distance as the B chain protein and therefore has approximately the same molecular weight; 10−30% ODA−PAA migrated further than the B chain protein and therefore has smaller molecular weight than the B chain protein. The PAA starting material has an average molecular weight of 1773 ± 1022 g/mol, so 10−30% ODA−PAA polymers has molecular weight approximately between 1775 and 2340 g/mol. Since this was the lowest molecular weight range protein panel that we could find, we cannot give more specific estimates on the molecular weights of these polymers. Fifty percent ODA−PAA migrated a shorter distance than the B chain protein, corresponding to a molecular weight between the third (aprotinin, 6.5 kDa) and fourth markers (lysozyme, 14.3 kDa). More important than these very rough molecular weight estimates is the trend observed in the polymer migration distances. We confirmed that with increasing degree of modification the migration distance is decreased and therefore the molecular weight increased. See Figure S4 in the Supporting Information.

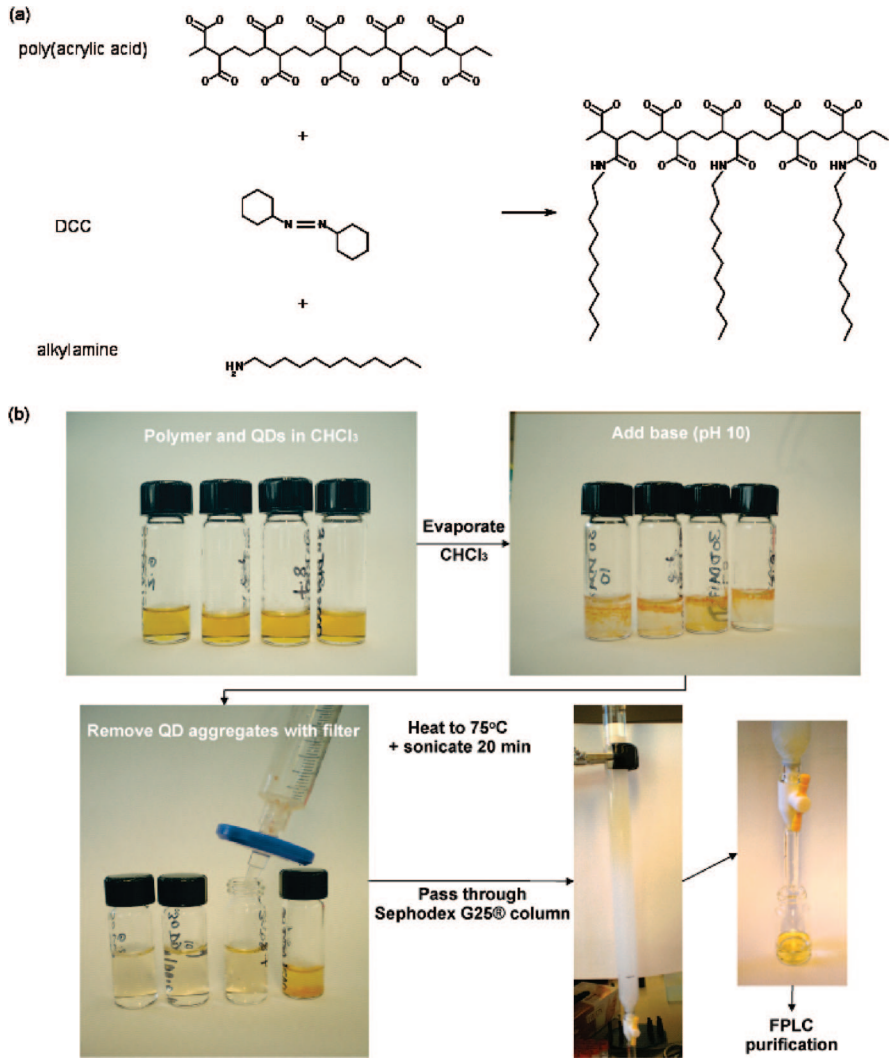

Figure 1. Schematic, preparation, and characterization of the amphiphilic polymer. (a) DCC conjugation of alkylamine to poly(acrylic acid). R = octyl, dodecyl, hexadecyl, or octadecyl group. (b) Overall procedure for coating QDs with modified poly(acrylic acid).

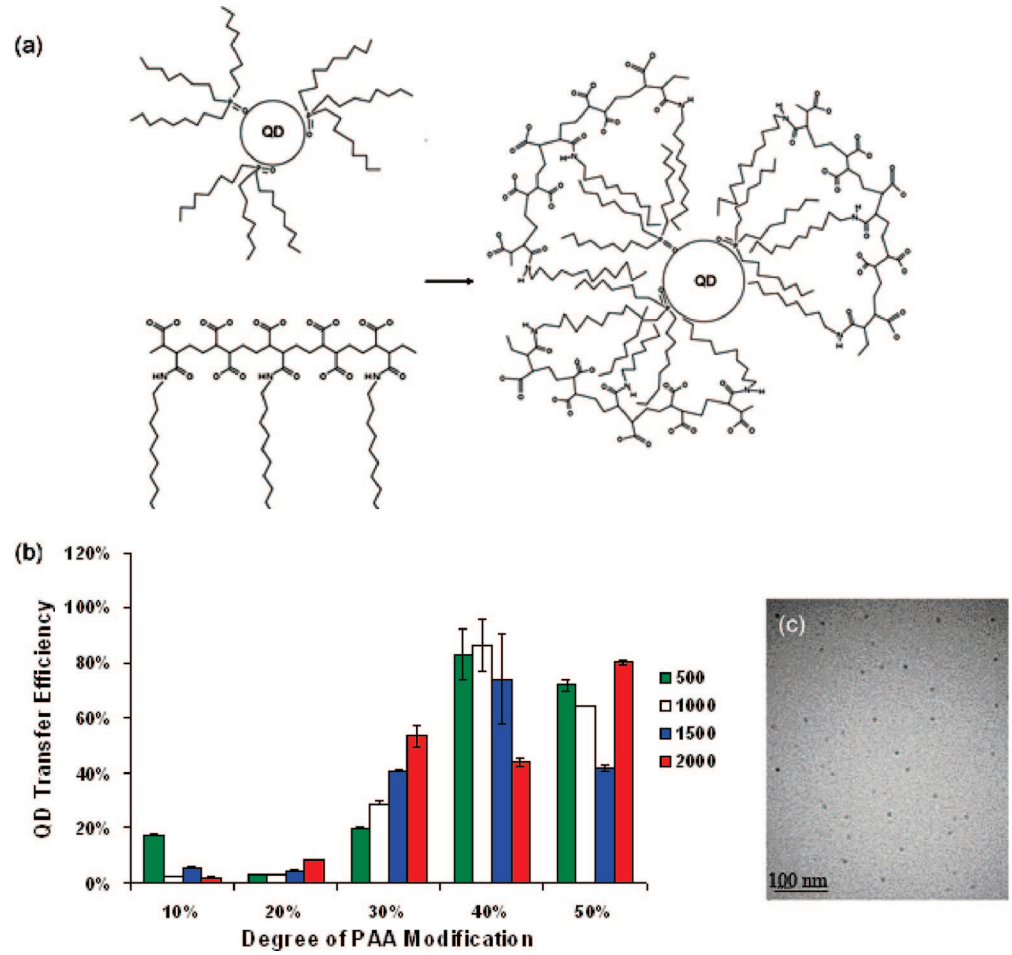

Figure 2. Surface modification and transfer efficiency of TOPO/HDA-stabilized QDs by wrapping with the amphiphilic polymer. (a) Proposed mechanism of QD polymer coating, (b) QD transfer efficiencies of the various modified polymers as determined by ICP-AES. QDs deemed as successfully transferred to water are soluble in this solvent and do not flocculate out of solution. (c) TEM image of red-emitting PQDs.

PQD Characterization. We assessed the transfer efficiency of the organic soluble CdSe/ZnS QDs to water by wrapping the surface ligands with an amphiphilic polymer. For a scheme of the overall coating procedure, see Figure 1b. In a general procedure, we mixed the polymer with the QDs dissolved in chloroform, evaporated the solvent, and followed with the addition of an aqueous buffer. We called these amphiphilic polymer-coated QDs (PQDs). See Figure 2a for a schematic of the coating. Three parameters were analyzed: (1) hydrophobic chain length (from 8 carbons to 18 carbons), (2) amount of hydrophobic chains per polymer (10−50%), and (3) ratio of polymer to QDs (500:1 to 2000:1); see Table 1 and Figure 2.

In order to identify the polymer that transfers the highest concentration of QDs between solvents, we used the technique of ICP-AES to measure Cd concentration before and after modification. The ratio is used to determine transfer efficiency. Table 1 shows all of the transfer efficiency. In our study, we discovered this process could lead to QD aggregations and hence during the purification process a large percentage of PQDs are lost. During the filtration process, large PQDs could be trapped in the membrane or polymer aggregates could trap smaller PQDs. Our estimation shows that as much as 51% could be lost in this process. In post-filtration, we observed that size exclusion chromatography could remove another 3−26%. To determine the total transfer efficiencies of the various polymers, the concentration of Cd in $CHCl_3$ was compared to that in the purified PQD solution in water.

In the initial part of the coating optimization study, we chose to use the yellow emitting QDs. The rationale being that they are ~4.5 nm and are in the middle of the size range for the ZnS-capped CdSe QD series. We used these results to narrow down the conditions for wrapping of the other QD sizes; otherwise, the number of permutations to completely and systematically optimize the coating scheme would be too great to conduct in a timely manner. Although this presentation of data is not typical in most research manuscripts, it is important to show the logic flow in optimizing these conditions since each research group or company could produce nanoparticles in different reaction conditions and hence slightly different chemistry. Our discussion should provide a practical guide to optimizing the surface modification.

TABLE 1. Specifications of the Various QDs (Size, Type, Ligands, *etc.*) and Polymers (Alkyl Chain Length and Degree of Modification) Used in Optimization Experiments, Along with the Range of Polymer to QD Ratios Used with the Resulting QD Transfer Efficiencies

QD specifications					specifications of examined polymers			
color	core size	QD type	surface ligands	emission wavelength	alkyl chain length	degree of modification	polymer: QD range	QD transfer efficiency range
yellow	3.9nm	CdSe/ZnS	TOPO/HAD	592nm	octyl (8)	10−50%	500−2000:1	2.6−13.5%
					dodecyl (12)	10−50%	10−3000:1	9.9−73.9%
					hexadecyl (16)	10−50%	500−2000:1	4.6−57.4%
					octadecyl (18)	10−50%	500−2000:1	28.9−55.2%
green	2.9nm	CdSe/ZnS	TOPO/HAD	542nm	dodecyl	30−50%	500−2000:1	4.4−83.0%
					hexadecyl	30−50%	500−2000:1	9.3−47.1%
					octadecyl	30−50%	500−2000:1	28.3−49.6%
red	6.0nm	CdSe/ZnS	TOPO/HAD	622nm	dodecyl	30−50%	500−3000:1	0.2−45.8%
					hexadecyl	30−50%	500−3000:1	0.5−5.3%
					octadecyl	30−50%	500−3000:1	7.3−96.0%
blue	2.0nm	CdSe/ZnS	TOPO/HAD	496nm	dodecyl	30−50%	500−2000:1	2.8−75.5%
					octadecyl	30−50%	500−2000:1	19.7−89.1%
N/R	5.5nm	CdTeSe/CdS	TOPO	722nm	dodecyl	40−50%	500−2000:1	1.5−9.2%
					octadecyl	40−50%	500−2000:1	1.6−97.0%

OA-modified polymers had the lowest PQD transfer efficiency at 2.6% (500:1, 40% OA−PAA) and the highest at 13.5 % (2000:1, 50% OA−PAA). The low transfer efficiencies suggest that ratios are not ideal for the water-solubilization process. For HDA−PAA polymer-produced PQDs, the lowest transfer efficiencies were 4.6% (500:1, 30% HDA−PAA) and the highest was 57.4 % (1750:1, 40% HDA−PAA). This is an improvement over the results for OA−PAAs but still was quite low. DDA−PAA polymers were used to yield PQD solutions with transfer efficiencies of 13.9% (500:1, 30% DDA−PAA) to 73.9% (500:1, 40% DDA−PAA). ODA−PAA polymers were used to yield PQD solutions with transfer efficiencies of 28.9% (1000:1, 30% ODA−PAA) to 55.2% (2000:1, 50% ODA−PAA).

We expanded the polymer to the yellow-emitting QD ratio range to confirm that the optimal value was within the ranges we had tested. Ratios of 10:1−3000:1 for 40% DDA−PAA were used. We selected 40% DDA−PAA for this study since it gave the highest transfer efficiency. The ratio of the polymer to QDs significantly affected the transfer efficiency. For example, at a ratio of 100:1, 250:1, and 2000:1, a transfer efficiency of 10, 32, and 74% was observed, respectively. However, as we increased beyond the 3000:1, we observed a slight decrease in transfer efficiency (see Figure S5 in Supporting Information). These results suggested that a minimum concentration of the polymer is needed in order to coat the QD surface (which contains TOPO and HDA ligands).

We further examined other QD nanoparticle sizes to determine if these parameters are universal for all QDs (blue to red emitting or 2.0 to 6.0 nm). On the basis of the results from the yellow-emitting QDs, we omitted OA−PAA polymers and 10−20 % modifications of all polymers since it led to poor transfer efficiencies. Thus, we characterized the transfer efficiencies for the 30−50% DDA−, HDA−, and ODA−PAA. Since the highest transfer efficiencies were found for ratios between 500:1 and 2000:1, that range was tested again.

For other intermediate sized green-emitting QDs, HDA−PAA PQD solutions with transfer efficiencies of 9.3% (500:1, 50% HDA−PAA) to 47.1% (2000:1, 40% HDA−PAA). DDA−PAA polymers were used to yield PQD solutions with transfer efficiencies of 4.4% (500:1 30% DDA−PAA) to 83.0 % (1000:1 40% DDA−PAA). ODA−PAA polymers were used to yield PQD solutions with transfer efficiencies of 28.3% (500:1 30% ODA−PAA) to 49.6% (500:1 40% ODA−PAA).

Next we examined the red-emitting QDs. These are the largest QDs, and the ratio range was therefore expanded to 500:1−3000:1. For red-emitting QDs, HDA−PAA PQD solutions had transfer efficiencies of 0.5% (1000:1 40% HDA−PAA) to 5.3% (2000:1 30% HDA−PAA). At this point, it was decided that HDA−PAA PQD did not have sufficient transfer efficiencies to be pursued in further investigations. DDA−PAA polymers were used to yield PQD solutions with transfer efficiencies of 0.2% (2500:1 50% DDA−PAA) to 45.8% (2000:1 50% DDA−PAA). ODA−PAA polymers were used to yield PQD solutions with transfer efficiencies of 7.3% (1000:1 30% ODA−PAA) to 96% (3000:1 40% ODA−PAA).

For the smallest QDs (which has blue emission), DDA−PAA polymers were used to yield PQD solutions with transfer efficiencies of 2.8% (500:1 50% DDA−PAA) to 75.5 % (2000:1 50% DDA−PAA). ODA−PAA polymers were used to yield PQD solutions with transfer efficiencies of 19.7% (500:1 50% ODA−PAA) to 89.1% (1000:1 40% ODA−PAA).

To determine if the polymer wrapping could be used for other types of QDs, we examined the ability of the polymer to solubilize near-IR-emitting alloyed CdS-capped $CdTe_xSe_{1-x}$ QDs. These QDs had the ligand

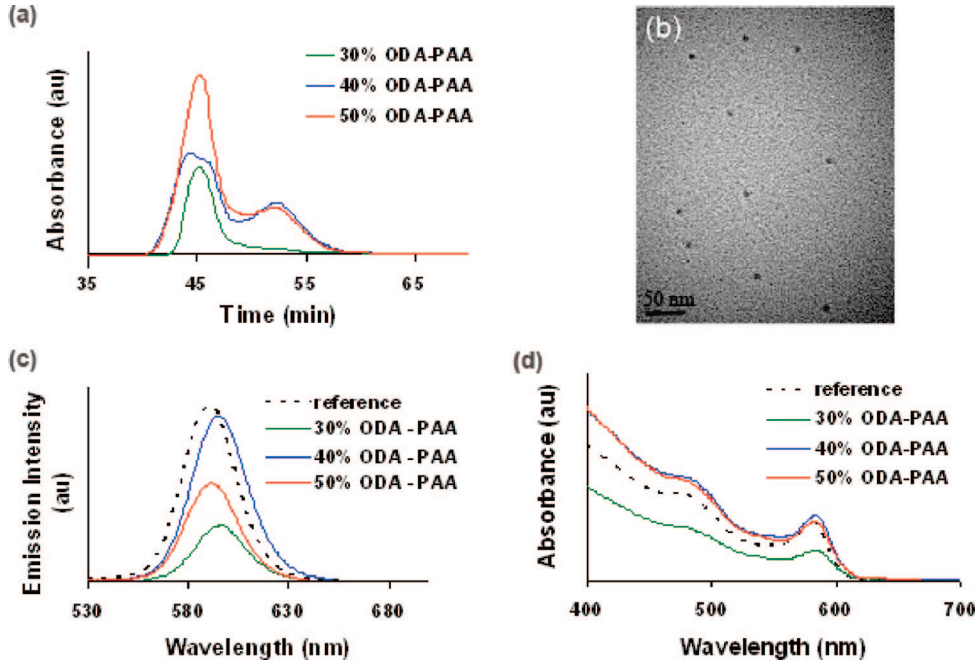

Figure 3. Analysis and characterization of the physical properties of the amphiphilic polymer-wrapped QDs (PQDs). (a) FPLC data for 30, 40, and 50% ODA−PAA PQD samples made from yellow-emitting QD with polymer:QD ratios of 500:1. (b) TEM image of small diameter fractions (scale bar = 50 nm). (c) Fluorescence spectra of 30% ODA−PAA PQD (15.4% QY), 40% ODA−PAA PQD (44.7% QY), and 50% ODA−PAA PQD (27.0% QY) samples made from yellow-emitting QD with polymer:QD ratios of 500:1 taken after 4 days with excitation at 522 nm. Reference (48.4% QY) is original QD solution in chloroform. (d) Absorbance spectra of 30, 40, and 50% ODA−PAA PQD samples made from yellow-emitting QD with polymer:QD ratios of 500:1. Reference is original QD solution in chloroform. AU refers to arbitrary units.

TOPO on its surface. The 50% ODA−PAA PQD had transfer efficiencies of 17−97% (500:1 and 1500:1, respectively). Meanwhile, 40% ODA−PAA and 40−50% DDA−PAA PQD solutions had transfer efficiencies that never exceeded 10%. The lowest was 1.6% for 1000:1 40% ODA−PAA, and the highest of the poor performing group was 9.2% for 2000:1 40% ODA−PAA.

Although each size QD had its own optimal polymer and polymer to QD ratio, we can make some general conclusions from the ICP data collected. Forty percent modification of PAA had slightly higher transfer efficiency than the 50% and much higher transfer efficiency than the 30%. All these combinations outperformed all of the 10−20% modifications. The PAAs that were modified with DDA and ODA had much higher transfer efficiencies than those modified with HDA, all of which outperformed OA−PAAs. The reason for DDA and ODA (12 and 18 carbon chain lengths, respectively) having higher transfer efficiencies than OA and HDA (8 and 16 carbon chain lengths, respectively) is not known, but we speculate that the exact matching of carbon chain lengths on the polymer to the carbon chain lengths on the QD surface ligands (TOPO chain length is 8 carbons long, HDA is 16) caused steric effects. Currently, there are several organic-based synthetic techniques to prepare QDs,[7,32–36] and one must consider the surface ligands on the QDs in order to effectively transfer the QDs between solvents. Of the different ratios investigated, 500:1−3000:1 is optimal for most QD sizes. Initially, we assumed that the smallest QD would require the least amount of polymer and the largest QD would require the most. However, we discovered that it was not straightforward. Although the red-emitting QDs tested do require the highest polymer:QD ratio, the yellow-emitting required the least, and green- and blue-emitting required a value between.

During this transfer process, we were surprised to discover that empty polymer micelles did not show up in the TEM images. This suggests that, during the purification process, the micelles were removed. However, if empty polymer micelles did form, as described by Dubertret *et al.*[12] and Luccardini *et al.*,[22] they could be removed by ultracentrifugation.

Size of PQDs after Modification. In addition to the removal of aggregates >15 nm in diameter, we used FPLC to probe the size and size distribution of the PQDs. As compared to gel electrophoresis, FPLC provided a higher resolution to identify size. We compared the retention time of the PQDs with that of proteins of known sizes to determine PQD size. Figure 3a shows typical chromatograms for analysis of yellow-emitting PQDs prepared by using different amphiphilic polymers. By comparing to standard protein sizes, the first peak (at $t \sim 45$ min) corresponds to PQD aggregates while the second peak ($t \sim 55$ min) corresponds to PQDs ~13 nms (see Figure S4 and Table S2 in Supporting Information). TEM imaging shows that PQDs eluted at ~45 min are small aggregates, while at 55 min they are single QDs (Figure 3b). By comparing the heights of the aggregate fraction peak to the height of the small diameter fraction (single PQD) peak, one can also estimate the relative amount of aggregate to single PQD in the original sample. For 40% ODA−PAA, 33.9% of the sample comprised single PQD. For 50% ODA−PAA, 20.4% of the sample comprised single PQD; 30% ODA−PAA yielded only an aggregate peak; 10 and 20% ODA−PAA-modified PQD did not have a sufficiently high enough concentration in water for analysis.

TEM images confirm the non-aggregated nature of the single PQD fraction. Since the polymer is difficult to visualize by this method, we could not use it to confirm the PQD radius. With TEM, the QD core is clearly vis-

ible but there is not enough contrast to image the thin polymer layer on the surface. To solve this, we used dynamic light scattering (DLS) measurements to approximate the hydrodynamic radius of the PQD. From our experience, DLS is an excellent technique to report the relative sizes of two nanoparticles; in many cases, the exact measurement of nanoparticle diameter is not reliable. QDs in $CHCl_3$ were found to be 9.7 nm. The same QDs after coating with 500:1 40% ODA−PAA and after all purification steps were 17.2 nm. These measurements are slightly larger than one might expect for QD and PQD given the FPLC data, which reported sizes of ~13 nm for PQD; however, the data confirm that the addition of the polymer increases the diameter of the particle. When comparing batches of PQDs made from the same QD core and coated with different polymer ratios, it was observed that the sizes of the PQDs did not vary significantly despite the amount of polymer used. This is not too surprising; once the surface is saturated with the amphiphilic polymer, we would not expect excess polymer to add to the overall size of the PQDs. All of the PQDs were larger than unmodified QDs, but all the PQDs were about the same size (16.9 ± 1.6 nm). Therefore, the ratio of polymer:QD does not directly correlate with the final size of the PQD, that is, more or less polymer does not necessarily equate to an overall larger or smaller PQD size, respectively. Interestingly, when Mattoussi and co-workers measured the size of commercial QDs coated with amphiphilic polymer, they observed a size of 30 ± 5 nm.[41] If we did not purify the PQDs using FPLC, our average size of the amphiphilic-coated QDs is similar to what Mattoussi *et al*. measured. Our study shows that the careful purification of these PQDs could lead to sub-15-nm nanoparticles.

The size of the QDs after modification is extremely important for many biomedical applications. As previously described by Frangioni *et al*.,[42] Nabiev *et al*.,[43] Zhang *et al*.,[44] and Fischer *et al*.,[45] nanoparticle size distribution is important in determining their pharmacokinetics in biotargeting applications. Chithrani *et al*.[46,47] demonstrated how size is important in cellular uptake of nanoparticles.

Optical Properties and Stability of PQDs. The optical properties of the PQDs were examined. After the water solubilization of yellow-emitting QDs with 40% ODA−PAA, the photoluminescence spectrum showed that the QY of the PQD is initially reduced compared to the QD in chloroform with a possible emission peak shift of ±5 nm. However, the QY increased 31−92% of the original after water solubilization when incubated in room temperature for 4 days. Photo-enhancement effects were also observed for PQDs modified with other polymer compositions, all improving 32 ± 6% from day 0 to day 4. Forty percent modified PAA produces the highest transfer efficiency (from ICP-AES measurements) and QY results, followed by 50 and 30% (Figure 3c,d). After the photo-enhancement, the photoluminescence of the PQDs appeared to remain constant. Photo-enhancement process for QDs has been observed by others.[48–52]

The fluorescence of the PQDs is sensitive to temperature. The fluorescence decreased as temperature increased in a trend similar to that of the mercaptoundecanoic acid−lysine cross-linked QDs.[38] Interestingly, Colvin *et al*. reported temperature stability of their water-soluble QD.[15] It is not clear to us why there is a discrepancy in the results. However, we want to point out that many studies have demonstrated a temperature-dependent effect on QD fluorescence;[53–55] this property may be intrinsic to the QD itself. In a salt-less solution and pH of 4 to 13, these PQDs do not precipitate out of solution. They remained monodisperse for many months. However, they do aggregate in certain buffers (*e.g.*, TBE = 5 days, 20 mM PBS = 1 day, 10 mM PBS = >20 days). In buffers such as sodium bicarbonate (pH = 6.7), HEPES buffer (pH = 6.7), and citrate buffer (pH = 6.7), we observed the PQDs to be stable against aggregation for at least 20 days. Generally, we store the PQDs in distilled water or borate buffer (10 mM, pH = 10).

Protein Adsorption to PQDs. Currently, PQDs are mostly used in many biological and biomedical applications. Therefore, we evaluated PQD non-specific protein adsorption. This process could impact the biosensing capability of QDs, direct the biodistribution of the QDs, or affect the non-specific uptake of the QDs. However, there are limited studies on this topic thus far.

In this study, the non-specific binding of proteins to the PQD surface was evaluated using agarose gel electrophoresis. This established method is widely used to separate biomolecules and has more recently proven to be useful in separation of nanoparticles, as well.[41,56,57] Separation occurs based on the species' overall electrophoretic mobility, which is due to its charge and/or molecular weight. In this analytical scheme, the non-specific adsorption of proteins onto the PQDs can accelerate or retard the movement of the PQDs in a gel. The agarose gel assay was analyzed via two routes. First the gel was imaged using UV light. This excited the PQDs in the gel and caused them to fluoresce, revealing their migration positions. Second, the gel was stained using the Bradford reagent, which stained the proteins blue and revealed the proteins' migration positions. After allowing the protein bands to develop overnight, the gels are imaged using white light. By comparing the fluorescence signal with the blue staining, we observed whether or not the PQD migration was accelerated or retarded (which indicates whether or not the proteins are non-specifically adsorbed onto or interact with the QD surface).

If a sample is completely homogeneous, then the resulting band is a thin dark line. It is obvious from the band shape of the PQD samples that there is some de-

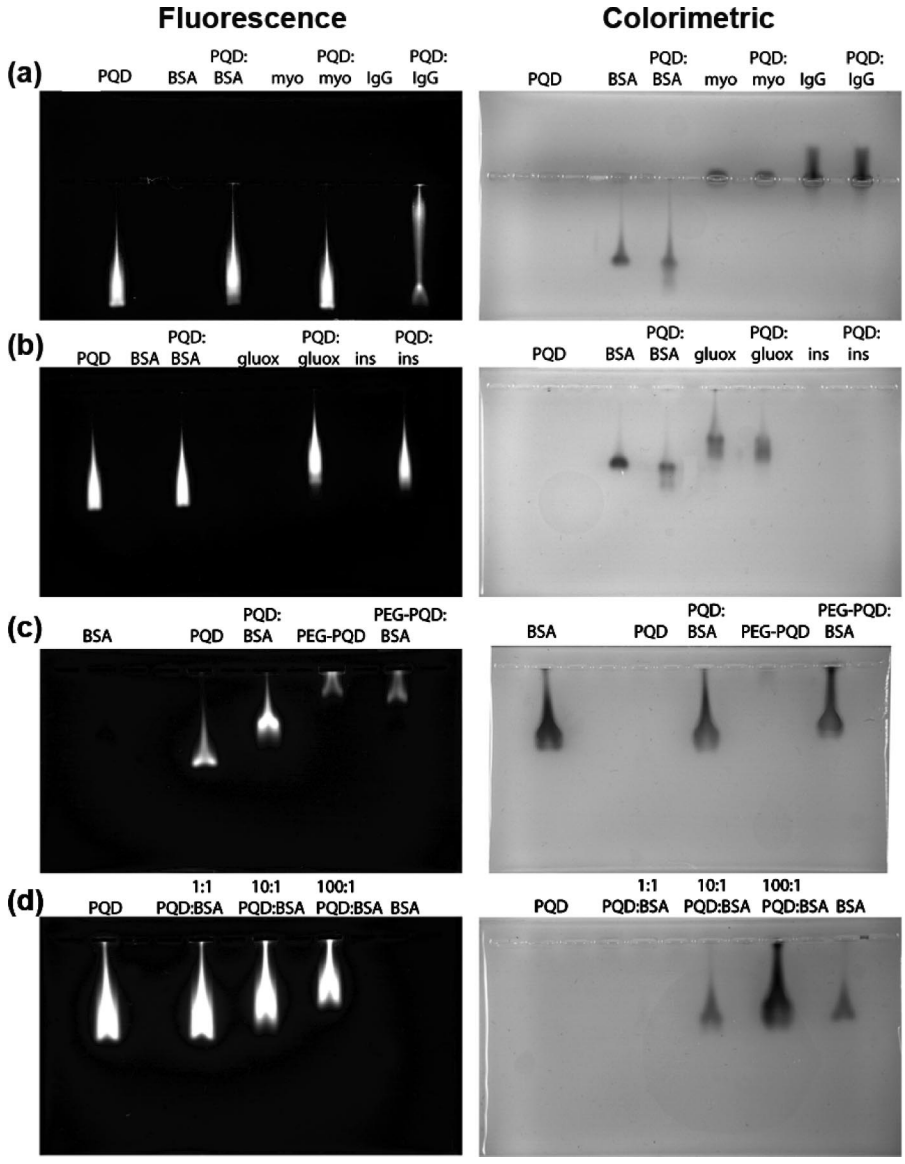

Figure 4. Non-specific protein binding to PQD. The fluorescence images of the agarose gels illustrate the effect of non-specifically bound proteins on the migration of PQD. The colorimetric images were stained with Bradford reagent in order to visualize the protein migration positions. (a) Effect of proteins of various isoelectric points on the migration of PQDs. The PQD:protein ratio is 1:10 for each. While myoglobin (pI 7.2) has no observable effect on PQD migration, BSA (pI 4.7) slows the migration of the PQD, and IgG (pI 9) slows the migration to an even greater degree. (b) Effect of proteins of similar isoelectric points (pI 4−5) on the migration of PQDs. The PQD:protein molar ratio is 1:10 for each. PQD migration distances were slowed the most by glucose oxidase (pI 4.2), slightly less by insulin (pI 5.4), and the least by BSA. (c) Investigating the effect of surface chemistry on protein non-specific binding, PQD and PEGlyated PQD (PEG−PQD) were mixed with BSA at 1:100. PEG−PQD reduces BSA non-specific binding compared to PQD. (d) With increasing protein concentrations (1:1, 1:10, and 1:100 PQD:BSA), the PQD migration is increasingly slowed.

gree of heterogeneity in the size of the PQDs, shown by the "smearing" in many of the bands. This smearing of PQDs in agarose gel analysis has been observed by others.[22] This suggests that not all the QDs have the same number of polymer strands wrapped around them, resulting in heterogeneity of weights or a shift in the overall charge of the nanoparticle. Since the PQD band is smeared, it is understandable that the subsequent protein−PQD bands would be smeared, as well. Also, smearing in protein−PQD samples may be increased over PQD samples if the same number of protein molecules do not attach to each PQD. Regardless, to compare the samples, we focused on the most concentrated, or darkest, portion of the band.

We initially examined the effect of protein isoelectric points (pI) on the non-specific absorption to PQD. To assess the effect of absorbed proteins with different isoelectric points, we incubated three proteins (BSA, myoglobin, IgG) of differing pI to PQD at a molar ratio of 1:10. We expected that, with increasing pI value, the protein would increasingly retard the movement of the PQD. BSA has a pI 4.7 and is negatively charged in 0.5× TBE buffer; therefore, it will move in the negative direction. BSA−PQD migration is retarded 9% compared to PQD alone and accelerated 45% compared to BSA alone. Myoglobin has a pI of 7, is neutral in 0.5× TBE, and should not migrate once current is applied. When PQDs are incubated with myoglobin, the PQD and myoglobin mobilities remain independent of each other. This is observed in Figure 4a. If any had absorbed onto the PQD surface, then either the PQD migration or the myoglobin migration would have been affected, but neither were. IgG with a pI of 9 is positively charged in the chosen buffer conditions and migrates in the negative direction. IgG−PQD migration is retarded 18% compared to PQD alone, and protein mobility is accelerated 10% in the positive direction compared to IgG alone. IgG (+ charge) had the most effect on PQD mobility, and BSA (− charge) had less effect than IgG but more effect than myoglobin (neutral).

To determine if proteins with similar pI values had similar non-specific binding to PQD, we analyzed the non-specific adsorption of a second set of proteins (*e.g.*, BSA, glucose oxidase, and insulin). These proteins have about the same pI, and all are negatively charged in 0.5× TBE and move in the positive direction. We incubated these proteins with PQD at 10:1 molar ratio. BSA−PQD migration is retarded 5% compared to PQD alone and accelerated 4% compared to BSA alone. Glucose oxidase has a pI of 4.2 and a slightly slower migration than that of BSA (Figure 4b). Its effect on PQD migra-

tion is to retard it by 29% compared to PQD alone and accelerate it by 9% compared to glucose oxidase alone. Glucose oxidase retarded the PQD mobility more than BSA did. Insulin with a pI of 5.4 retards insulin−PQD migration by 24% compared to PQD alone. Figure 4b shows insulin had little effect on PQD mobility. We can conclude that proteins with similar pI values could elicit different effects on PQD mobility, suggesting that the interactions of the proteins to PQDs are not necessarily dictated by charge. Although insulin at this concentration does not react with the Bradford reagent sufficiently to produce a visible stain, a higher insulin concentration was also examined to determine mobility. A 100:1 insulin:PQD was needed in order for the staining to be effective, but even at that concentration, the protein−PQD mobility remained unchanged.

While these previous experiments showed that non-specific binding is not dependent on protein isoelectric point, we wanted to evaluate whether it is dependent on the nature of the PQD surface. PEGylation is an established method used to reduce non-specific binding of proteins[58,59] and has also been employed to reduce non-specific binding of QD.[60] Predictably, compared to PQD, the non-specific binding of PEGylated PQD (PEG−PQD) to BSA is reduced (Figure 4c). PEGylation of PQD was carried out via EDC coupling of PQD with amine-terminated PEG. DLS measurements show an increase in PQD size to 21.2 nm after PEGylation. Evidence of successful conjugation can be observed by the marked decrease in migration distance of PEG−PQD compared to PQD as a result of the added bulk of PEG. The migration distance was so retarded that it was shorter than the BSA migration distance. Any adsorption of BSA onto PEG−PQD would therefore have the opposite effect on PQD; that is, BSA−PEG−PQD should be accelerated while BSA−PQD would be retarded. The degree of adsorption can be estimated by comparing the distance accelerated or retarded to the original migration distance without BSA. BSA−PQD is retarded by 40%, and BSA−PEG−PQD is accelerated by 25%. We can conclude that the PQD migration is more affected by BSA incubation than PEG−PQD. Therefore, in future work involving solutions of high protein concentration, PEGylation of the PQD should be employed to reduce non-specific protein binding.

Another important factor to take into account was the effect of protein concentration on protein−PQD migration. For these studies, we used BSA as a model protein. The gel imaged in Figure 4d illustrates how an increasing BSA concentration (1:1, 10:1, 100:1) influenced PQD migration. The migration distance of BSA:PQD 1:1 is retarded by 6% compared to PQD alone. For 10:1, the migration distance was retarded by 24% and for 100:1 by 44% (compared to PQD alone). For both 10:1 and 100:1 cases, BSA−PQD was accelerated compared to BSA alone by 11%. The 1:1 BSA concentration was too low for this staining method to be effective. We speculate that the concentration of the protein affects the degree of saturation on the QD surface.

Many factors appear to dictate the non-specific adsorption of the PQDs with proteins. Clearly these results indicate that the non-specific adsorption is dependent upon the protein and that it is difficult to predict the types of proteins that will adsorb onto the PQDs. Properties of the proteins such as charge and hydrophobicity are important in the adsorption process. Further, the overall surface modification of the PQDs influences the non-specific adsorption; for example, the PEGylation of the PQD's surface reduced the degree of non-specific binding. More studies will be required to completely understand the physical−chemical relationship between protein properties and non-specific interactions.

CONCLUSIONS

In conclusion, we systematically optimized the modification of the organic-soluble QDs with amphiphilic polymers. This is an important step to their broad utility in biomedical applications. This systematic approach could be applied toward surface modification and characterization of other nanostructures. We provide detailed synthesis and characterization of a variety of modified PAA polymers. We found the preferred polymer modification and optimal molar ratio for each of four TOPO-HDA-stabilized ZnS-capped CdSe QD sizes and for TOPO-stabilized CdS-capped $CdTe_xSe_{1-x}$ QDs. Generally, 40 and 50% ODA− and DDA−PAA at ratios of 500:1 to 3000:1 are the most efficient for solubilizing blue to red and near-infrared emitting QDs. In the future, this optimization method can serve as a guideline for determining the most efficient polymer and ratio for solubilization of QDs of various types and with diverse surface ligands. More specifically, using the optimized parameters, we obtained transfer efficiencies of 96% for red-emitting QD solubilized by 3000:1 40% ODA−PAA, 74% for yellow-emitting by 500:1 40% DDA−PAA, 83% for green-emitting by 1000:1 40% ODA−PAA, 89% for blue-emitting by 500:1 50% ODA−PAA, and 97% for NIR-emitting by 1500:1 50% ODA−PAA. These PQDs are stable over a pH range of 4−13, for many months, and retained up to 92% of the QY of the starting QD solution.

For many biological applications, the degree of non-specific protein adsorption dictates the usefulness of the QDs. Thus, we found that the non-specific adsorption is dependent upon the protein itself and that it is difficult to predict the types of proteins that non-specifically adsorbed onto the PQD surface based solely on their isoelectric points. Hydrophobicity, charge, and concentration of the proteins undoubtedly play a role in determining absorption to PQD. However, the PQDs could be PEGylated to reduce the degree of non-specific binding.

METHODS

Reagents. Poly(acrylic acid) (PAA), 1-methyl-2-pyrrolidinone (MPD), 1,3-dicyclohexylcarbodiimide (DCC), octylamine (OA), dodecylamine (DDA), hexadecylamine (HDA), octadecylamine (ODA), rhodamine 6G, Bradford reagent, myoglobin, glucose oxidase, tri-*n*-octyphosphine oxide (TOPO), ninhydrin, phosphate buffered saline tablets (PBS), *N*-(3-dimethylaminopropyl)-*N*′-ethylcarbodiimide hydrochloride (EDC), and bovine serum albumin (BSA) were all purchased from Sigma-Aldrich (St. Louis, MO). *O*-(2-Aminoethyl)polyethylene glycol 3000 (PEG) was purchased from Fluka (Germany). Agarose was purchased from EMD Chemical, Inc. (Gibbstown, NJ). The 10× tris-borate-EDTA electrophoresis buffer (TBE) was purchased from Fermentas (Lithuania). Anti-goat mouse IgG and Gelcode blue stain reagent were purchased from Pierce (Rockford, IL). The broad range (2−212 kDa) protein marker was purchased from New England Biolabs (Ipswich, MA). All chemicals were used as received.

Amphiphilic Polymer Synthesis and Characterization. We provide an example of synthesizing 40% octadecylamine-modified PAA. All other amphiphilic polymers used in the study were synthesized in a similar manner, but the molar ratio of alkylamine molecule to PAA was adjusted for the desired % modification. For preparing these polymers, a slight modification of a procedure[40] was used; 0.0695 mol of PAA (~1800 g/mol molecular weight) was dissolved in 150 mL of MPD at 60 °C for 24 h under constant stirring. In a separate reaction vessel, 0.0278 mol of DCC was dissolved in 10 mL of MPD, added to the PAA solution, and allowed to react for 1 h at 60 °C under constant stirring. Finally, 0.0278 mol of ODA was dissolved in 10 mL of MPD, added to the PAA−DCC solution, and allowed to react for 24 h at 60 °C under constant stirring. The solution was then cooled to room temperature and filtered through Whatman filter paper (Fischer Scientific Canada, Ottawa, ON) to remove any unwanted dicyclohexylurea crystal byproducts. Afterward, 0.0278 mol of NaOH was added to induce polymer precipitation, and this was followed by centrifugation (3700 rpm, 5 min). The supernatant was discarded, and the pellet was washed with hot MPD (60 °C) and methanol to remove any impurities. The final solid was dried overnight and stored at room temperature prior to use in quantum dot experiments. As a first mode of characterization, FTIR spectroscopy (Thermo Nicolet Nexus 670 FT-0IR, Waltham, MA) was used to verify the formation of an amide bond, which indicates a successful reaction between the alkylamine with the PAA. A similar method was used to prepare the 10−50% OA, DDA, HDA, and ODA modifications of PAA.

We determined the degree of modification of the PAA by the alkylamine using a triketohydrindane hydrate assay, which is commonly known as a ninhydrin assay. Ninhydrin reacts with primary or secondary amine to form a blue color ammonium salt that could be quantitated using spectrophotometry, and the measurements could be equated to the concentration of the amine-containing molecules. In all of our amphiphilic polymer preparations, we used ninhydrin to measure the concentration of the alklyamine before and after the reaction. From these data, we can determine the number of alkylamine that reacted to the PAA. For example, 56 μmol of ninhydrin was added to an ethanol solution containing octyldecylamine (0.00278) and PAA (average MW of 2000 g/mol, 0.00694), and the reaction was allowed to occur overnight. Afterward, the sample was placed into a spectrophotometer (Tecan Sunrise microplate reader, Switzerland), and an absorbance value was obtained at 570 and 700 nm. The value at 700 nm was used as a reference standard. Using $\epsilon = 0.3556\ mM^{-1}\ cm^{-1}$, a concentration was determined using Beer's law ($A = \epsilon bc$, where A is the absorbance value, ϵ is the molar absorptivity value, b is the path length, and c is the concentration). By determining the concentration of alkylamine before and after the reaction, we can determine the percentage of carboxylic acids on the PAA reacted to the alkylamine.

After modification, we further characterized the molecular weight of the polymer using agarose gel electrophoresis. A 3% agarose gel was prepared using standard techniques. We added to the lanes the polymers plus a protein biomarker panel (New England Biolabs, Ipswich, MA). This panel contained proteins in the size range of 2−212 kDa. The gel was run in 0.5× TBE buffer (pH = 8.4) for 30 min at 100 mV. Afterward, the gel was soaked in Gelcode blue stain reagent (Rockford, IL) and imaged using the Biorad Gel Doc XR (Hercules, CA) with white light to visualize the polymers and proteins. A comparison of polymer migration rate to that of the proteins was used to estimate the molecular weight. We also attempted to use ^{1}HNMR and MALDI-MS for assessing molecular weight but did not find much success (see Figure S2 in Supporting Information).

Coating Quantum Dots with Amphiphilic Polymers (PQD). We used ZnS-capped CdSe QDs coated with TOPO and HDA surface ligands and CdS-capped $CdTe_{1-x}Se_x$ near-infrared-emitting (NIR) QDs with TOPO surface ligands for this study. We synthesized these QDs according to previously reported methods with a slight modification.[7,32,41] In contrast to previous studies, the TOPO and HDA (at a mass ratio of 1.4:1.0) was used as the solvent to prepare the QDs. For our synthesis, we observed that this ligand combination produced bright QDs. After synthesis, QD concentrations were determined using Beer's law after measuring the absorbance value using spectrophotometry. We used the reported molar absorptivity value for QDs.[61]

Using the 40% ODA−PAA, we provide a typical procedure for modification of the QDs. The overall procedure for coating QDs with alkylamine-reacted poly(acrylic acid) is shown in Figure 1; 40% ODA−PAA (0.45 μmol) and ZnS-capped CdSe QDs (0.0015 mol) were dissolved in $CHCl_3$ and stirred continuously for 1 h in a closed container, followed by air evaporation in a fume hood. Afterward, distilled water and NaOH were added to the reaction flask until a pH of 10 was reached. The reaction flask was then sonicated for 30 min, heated to 75 °C for 10 min, sonicated for another 5 min, and filtered through a 0.22 μm Millipore syringe filter (Fisher Scientific, Ottawa, ON). The filtration removed excess polymers and QD aggregates. We further purified the polymer-coated QDs (PQDs) using size exclusion chromatography (Sephadex G25). In some cases, further purification *via* a fast protein liquid chromatography (FPLC) system may be needed to narrow the size distribution. Table 1 describes the size, QD type, polymers, and QD-to-polymer ratio used in this study.

After purification, the optical properties were measured using UV−visible and fluorescence spectroscopy (Jobin-Yvon Fluoromax-3, Edison, NJ). We further used transmission electron microscopy, TEM (Phillips FEI CM100 system, Hillsboro, OR), to determine the monodispersity and size of the core−shell QDs. These characterization procedures are described in our previous publications. For assessment of the size of the QDs with polymer coating (PQDs), we used two methods. The PQDs were injected into the FPLC system, and elution time of the PQDs was compared to the elution time of the protein marker panel (ferritin, catalase, aldolase, bovine serum albumin, α-chymotrypsin, and ribonuclease A) of known size (see Figure S4 in Supporting Information). We used a HiLoad 16/60 superdex 200 prep grade column (AKTA fast protein liquid chromatography (FPLC), GE Amersham Biosciences, Piscataway, NJ), which consists of 34 μm beads of highly cross-linked agarose covalently bound to dextran. It has a molecular weight separation range of 10−60 kDa. For each sample analyzed, 1 mL of concentrated PQD solution was run through the column at a flow rate of 1 mL/min. In this analysis, a UV detector (280 nm) was used to assess concentration and samples were collected. We further verified the size of the PQDs by using dynamic light scattering (Malvern Zetasizer Nano-ZS, Worcestershire, UK) as described previously.[38,41]

To assess concentration, UV−vis spectroscopy could be used because the adsorption of light by the polymer interfered with the signal. For PQDs, we used the technique of inductively coupled plasma-atomic emission spectroscopy (Perkin Elmer Optima 3000 ICP AES, Waltham, MA). ICP-AES was used to determine Cd concentration, which could be correlated to the PQD concentration. For procedural details, see refs 45 and 62.

Assessing Protein Adsorption onto PQD Surface. In these experiments, we assessed how proteins of different isoelectric point (IgG and myoglobin) and different composition affected nonspecific binding onto QD surface. We studied two surfaces: amphiphilic polymer coated and polyethylene glycol (PEG) coated.

PEG coated onto the PQDs were prepared using an EDC reaction. In the reaction scheme, a final molar ratio of 1:500:4000 PQD:amino-PEG:EDC in PBS (10 mM, pH 7.4) was mixed in a reaction vial and allowed to react at room temperature for 30 min

and followed by purification through a Sephadex G25 column. The PEG−PQD conjugates were compared to unconjugated PQD in a gel electrophoresis assay (a successful conjugation shows a shift in the migration rate).

In a typical protein absorption experiment, we dissolved the PQDs in 0.5× Tris-borate EDTA buffer and added the protein bovine serum albumin (BSA), followed by incubation at 37 °C for 30 min. Afterward, the samples were analyzed using agarose gel electrophoresis (1% in 0.5× TBE buffer, 30 min, 100 mV). We analyzed the gel using UV light to determine PQD position, and then we stained the gel with Bradford reagent to determine protein position. Similar studies were done with myoglobin, immunoglobulin G (IgG), glucose oxidase (gluox), and insulin (ins).

Acknowledgment. The authors thank Genome Canada through the Ontario Genome Institute, Canadian Institute of Health Research, Canadian Foundation for Innovation, and Ontario Innovative Trust for funding, Wen Jiang for helpful discussions and synthesis of CdS-capped $CdTe_xSe_{1-x}$ QD, David Li for ZnS-capped CdSe QD synthesis, Hans Fischer for PEG conjugation, and Dr. Ian Corbin in Zheng's lab at University Health Network for FPLC measurements.

Supporting Information Available: Explanation of zetasizer measurements, representative polymer mass spectra, ninhydrin assay standard curve and data for octadecylamine, agarose gel of polymers estimating their molecular weights, and FPLC standard curve and data. This material is available free of charge *via* the Internet at http://pubs.acs.org.

REFERENCES AND NOTES

1. Burda, C.; Chen, X.; Narayanan, R.; El-Sayed, M. A. Chemistry and Properties of Nanocrystals of Different Shapes. *Chem. Rev.* **2005**, *105*, 1025–1102.
2. Park, J.; Joo, J.; Kwon, S. G.; Jang, Y.; Hyeon, T. Synthesis of Monodisperse Spherical Nanocrystals. *Angew. Chem., Int. Ed.* **2007**, *46*, 4630–4660.
3. Tenne, R. Advances in the Synthesis of Inorganic Nanotubes and Fullerene-Like Nanoparticles. *Angew. Chem., Int. Ed.* **2003**, *42*, 5124–5132.
4. Cozzoli, P. D.; Manna, L. Asymmetric Nanoparticles: Tips on Growing Nanocrystals. *Nat. Mater.* **2005**, *4*, 801–802.
5. Duan, H.; Nie, S. Cell-Penetrating Quantum Dots Based on Multivalent and Endosome-Disrupting Surface Coatings. *J. Am. Chem. Soc.* **2007**, *129*, 3333–3336.
6. Lalatonne, Y.; Richardi, J.; Pileni, M. P. Van Der Waals Versus Dipolar Forces Controlling Mesoscopic Organizations of Magnetic Nanocrystals. *Nat. Mater.* **2004**, *3*, 121–125.
7. Peng, Z. A.; Peng, X. G. Formation of High-Quality CdTe, CdSe, and CdS Nanocrystals Using Cdo as Precursor. *J. Am. Chem. Soc.* **2001**, *123*, 183.
8. Wiley, B. J.; Chen, Y.; McLellan, J. M.; Xiong, Y.; Li, Z.-Y.; Ginger, D.; Xia, Y. Synthesis and Optical Properties of Silver Nanobars and Nanorice. *Nano Lett.* **2007**, *7*, 1032–1036.
9. Chan, W. C. W.; Nie, S. Quantum Dot Bioconjugates for Ultrasensitive Nonisotopic Detection. *Science* **1998**, *281*, 2016–2018.
10. Freeman, R. G.; Grabar, K. C.; Allison, K. J.; Bright, R. M.; Davis, J. A.; Guthrie, A. P.; Hommer, M. B.; Jackson, M. A.; Smith, P. C.; Walter, D. G. Self-Assembled Metal Colloid Monolayers: An Approach to Sers Substrates. *Science* **1995**, *267*, 1629–1632.
11. Mattoussi, H.; Mauro, M. J.; Goldman, E. R.; Anderson, G. P.; Sundar, V. C.; Mikulec, F. V.; Bawendi, M. G. Self-Assembly of Cdse-Zns Quantum Dot Bioconjugates Using an Engineered Recombinant Protein. *J. Am. Chem. Soc.* **2000**, *122*, 12142–12150.
12. Dubertret, B.; Skourides, P.; Norris, D. J.; Noireaux, V.; Brivanlou, A. H.; Libchaber, A. *In Vivo* Imaging of Quantum Dots Encapsulated in Phospholipid Micelles. *Science* **2002**, *298*, 1759–1762.
13. Pellegrino, T.; Manna, L.; Kudera, S.; Liedl, T.; Koktysh, D.; Rogach, A. L.; Keller, S.; Radler, J.; Natile, G.; Parak, W. J. Hydrophobic Nanocrystals Coated with an Amphiphilic Polymer Shell: A General Route to Water Soluble Nanocrystals. *Nano Lett.* **2004**, *4*, 703–707.
14. Wu, X.; Liu, H. J.; Liu, J. Q.; Haley, K. N.; Treadway, J. A.; Larson, J. P.; Ge, N. F.; Peale, F.; Bruchez, M. P. Immunofluorescent Labeling of Cancer Marker Her2 and Other Cellular Targets with Semiconductor Quantum Dots. *Nat. Biotechnol.* **2003**, *21*, 41–46.
15. Yu, W. W.; Chang, E.; Falkner, J. C.; Zhang, J.; Al-Somali, A. M.; Sayes, C. M.; Johns, J.; Drezek, R.; Colvin, V. L. Forming Biocompatible and Nonaggregated Nanocrystals in Water Using Amphiphilic Polymers. *J. Am. Chem. Soc.* **2007**, *129*, 2872–2879.
16. Darbandi, M.; Thomann, R.; Nann, T. Single Quantum Dots in Silica Spheres by Microemulsion Synthesis. *Chem. Mater.* **2005**, *17*, 5720–5725.
17. Gao, X.; Nie, S. Doping Mesoporous Materials with Multicolor Quantum Dots. *J. Phys. Chem. B* **2003**, *107*, 11575–11578.
18. Han, M.; Gao, X.; Su, J. Z.; Nie, S. Quantum-Dot-Tagged Microbeads for Multiplexed Optical Coding of Biomolecules. *Nat. Biotechnol.* **2001**, *19*, 631–635.
19. Schabas, G.; Yusuf, H.; Moffitt, M. G.; Sinton, D. Controlled Self-Assembly of Quantum Dots and Block Copolymers in a Microfluidic Device. *Langmuir* **2008**, *24*, 637–643.
20. Smith, A. M.; Duan, H.; Rhyner, M. N.; Ruan, G.; Nie, S. A Systematic Examination of Surface Coatings on the Optical and Chemical Properties of Semiconductor Quantum Dots. *Phys. Chem. Chem. Phys.* **2006**, *8*, 3895–3903.
21. Nann, T. Phase-Transfer of Cdse@Zns Quantum Dots Using Amphiphilic Hyperbranched Polyethylenimine. *Chem. Commun.* **2005**, 1735–1736.
22. Luccardini, C.; Tribet, C.; Vial, F.; Marchi-Artzner, V.; Dahan, M. Size, Charge, and Interactions with Giant Lipid Vesicles of Quantum Dots Coated with an Amphiphilic Macromolecule. *Langmuir* **2006**, *22*, 2304–2310.
23. Wang, M.; Felorzabihi, N.; Guerin, G.; Haley, J. C.; Sechloes, G. D.; Winnik, M. A. Watersoluble CdSe Quantum Dots Passivated by a Multidentate Diblock Copolymer. *Macromolecules* **2007**, *40*, 6377–6384.
24. Asuri, P.; Bale, S. S.; Karajanagi, S. S.; Kane, R. S. The Protein−Nanomaterial Interface. *Curr. Opin. Biotechnol.* **2006**, *17*, 562–568.
25. Derfus, A. M.; Chan, W. C. W.; Bhatia, S. N. Probing the Cytotoxicity of Semiconductor Quantum Dots. *Nano Lett.* **2004**, *4*, 11–18.
26. Gopalakrishnan, G.; Danelon, C.; Izewska, P.; Prummer, M.; Bolinger, P.-Y.; Geissbühler, I.; Demurtas, D.; Dubochet, J.; Vogel, H. Multifunctional Lipid/Quantum Dot Hybrid Nanocontainers for Controlled Targeting of Live Cells. *Angew. Chem., Int. Ed.* **2006**, *45*, 5478–5483.
27. Kirchner, C.; Liedl, T.; Kudera, S.; Pellegrino, T.; Javier, A. M.; Gaub, H. E.; Stolzle, S.; Fertig, N.; Parak, W. J. Cytotoxicity of Colloidal CdSe and CdSe/ZnS Nanoparticles. *Nano Lett.* **2005**, *5*, 331–338.
28. Bruchez, M.; Moronne, M.; Gin, P.; Weiss, S.; Alivisatos, A. P. Semiconductor Nanocrystals as Fluorescent Biological Labels. *Science* **1998**, *281*, 2013–2016.
29. Gao, X.; Yang, L.; Petros, J. A.; Marshall, F. F.; Simons, J. W.; Nie, S. *In Vivo* Molecular and Cellular Imaging with Quantum Dots. *Curr. Opin. Biotechnol.* **2005**, *16*, 63–72.
30. Klostranec, J. M.; Chan, W. C. W. Quantum Dots in Biological and Biomedical Research: Recent Progress and Present Challenges. *Adv. Mater.* **2006**, *18*, 1953–1964.
31. Medintz, I. L.; Uyeda, H. T.; Goldman, E. R.; Mattoussi, H. Quantum Dot Bioconjugates for Imaging, Labelling and Sensing. *Nat. Mater.* **2005**, *4*, 435–446.
32. Dabbousi, B. O.; Rodriguez-Viejo, J.; Mikulec, F. V.; Heine, J. R.; Mattoussi, H.; Ober, R.; Jensen, K. F.; Bawendi, M. G. (CdSe)ZnS Core−Shell Quantum Dots: Synthesis and Characterization of a Size Series of Highly Luminescent Nanocrystallites. *J. Phys. Chem. B* **1997**, *101*, 9463–9475.
33. Hines, M. A.; Guyot-Sionnest, P. Synthesis and Characterization of Strongly Luminescing ZnS Capped CdSe Nanocrystals. *J. Phys. Chem.* **1996**, *100*, 468–471.

34. Peng, X. Green Chemical Approaches toward High-Quality Semiconductor Nanocrystals. *Chem.—Eur. J.* **2002**, *8*, 335–339.
35. Peng, X.; Schlamp, M. C.; Kadavanich, A. V.; Alivisatos, A. P. Epitaxial Growth of Highly Luminescent CdSe/CdS Core/Shell Nanocrystals with Photostability and Electronic Accessibility. *J. Am. Chem. Soc.* **1997**, *119*, 7019–7029.
36. Qu, L.; Peng, Z. A.; Peng, X. Alternative Routes toward High Quality CdSe Nanocrystals. *Nano Lett.* **2001**, *1*, 333–337.
37. Jaiswal, J. K.; Mattoussi, H.; Mauro, J. M.; Simon, S. M. Long-Term Multiple Color Imaging of Live Cells Using Quantum Dot Bioconjugates. *Nat. Biotechnol.* **2003**, *21*, 47–51.
38. Jiang, W.; Mardyani, S.; Fischer, H.; Chan, W. C. W. Design and Characterization of Lysine Cross-Linked Mercapto-Acid Biocompatible Quantum Dots. *Chem. Mater.* **2006**, *18*, 872–878.
39. Chattopadhyay, P. K.; Price, D. A.; Harper, T. F.; Betts, M. R.; Yu, J.; Gostick, E.; Perfetto, S. P.; Goepfert, P.; Koup, R. A.; De Rosa, S. C. Quantum Dot Semiconductor Nanocrystals for Immunophenotyping by Polychromatic Flow Cytometry. *Nat. Med.* **2006**, *12*, 972–977.
40. Wang, K. T.; Iliopoulos, I.; Audebert, R. Viscometric Behaviour of Hydrophobically Modified Poly(Sodium Acrylate). *Polym. Bull.* **1988**, *20*, 577–582.
41. Pons, T.; Uyeda, H. T.; Medintz, I. L.; Mattoussi, H. Hydrodynamic Dimensions, Electrophoretic Mobility, and Stability of Hydrophilic Quantum Dots. *J. Phys. Chem. B* **2006**, *110*, 20308–20316.
42. Kim, S.; Lim, Y. T.; Soltesz, E. G.; De Grand, A. M.; Lee, J.; Nakayama, A.; Parker, J. A.; Mihaljevic, T.; Laurence, R. G.; Dor, D. M. Nearinfrared Fluorescent Type Ii Quantum Dots for Sentinel Lymph Node Mapping. *Nat. Biotechnol.* **2004**, *22*, 93–97.
43. Wargnier, R.; Baranov, A. V.; Maslov, V. G.; Stsiapura, V.; Artemyev, M.; Pluot, M.; Sukhanova, A.; Nabiev, I. Energy Transfer in Aqueous Solutions of Oppositely Charged CdSe/ZnS Core/Shell Quantum Dots and in Quantum Dot-Nanogold Assemblies. *Nano Lett.* **2004**, *4*, 451–457.
44. Zhang, Y.; Chen, W.; Zhang, J.; Liu, J.; Chen, G.; Pope, C. *In Vitro* and *In Vivo* Toxicity of CdTe Nanoparticles. *J. Nanosci. Nanotechnol.* **2007**, *7*, 497–503.
45. Fischer, H. C.; Liu, L.; Pang, K. S.; Chan, W. C. W. Pharmacokinetics of Nanoscale Quantum Dots: *In Vivo* Distribution, Sequestration, and Clearance in the Rat. *Adv. Funct. Mater.* **2006**, *16*, 1299–1305.
46. Chithrani, B. D.; Chan, W. C. W. Elucidating the Mechanism of Cellular Uptake and Removal of Protein-Coated Gold Nanoparticles of Different Sizes and Shapes. *Nano Lett.* **2007**, *7*, 1542–1550.
47. Chithrani, B. D.; Ghazani, A. A.; Chan, W. C. W. Determining the Size and Shape Dependence of Gold Nanoparticle Uptake into Mammalian Cells. *Nano Lett.* **2006**, *6*, 662–688.
48. Cordero, S. R.; Carson, P. J.; Estabrook, R. A.; Strouse, G. F.; Buratto, S. K. Photo-Activated Luminescence of CdSe Quantum Dot Monolayers. *J. Phys. Chem. B* **2000**, *104*, 12137–12142.
49. Jiang, W.; Singhal, A.; Zheng, J.; Wang, C.; Chan, W. C. W. Optimizing the Synthesis of Red- to near-Ir-Emitting CdS-Capped CdTe XSe1-X Alloyed Quantum Dots for Biomedical Imaging. *Chem. Mater.* **2006**, *18*, 4845–4854.
50. Manna, L.; Scher, E. C.; Li, L.; Alivisatos, A. P. Epitaxial Growth and Photochemical Annealing of Graded CdS/ZnS Shells on Colloidal CdSe Nanorods. *J. Am. Chem. Soc.* **2002**, *124*, 7136–7145.
51. van Sark, W.; Frederix, P.; Van den Heuvel, D. J.; Gerritsen, H. C.; Bol, A. A.; van Lingen, J. N. J.; Donega, C. D.; Meijerink, A. Photooxidation and Photobleaching of Single CdSe/ZnS Quantum Dots Probed by Room-Temperature Time-Resolved Spectroscopy. *J. Phys. Chem. B* **2001**, *105*, 8281–8284.
52. Yu, J.; Liu, H.; Wang, Y.; Fernandez, F. E.; Jia, W.; Sun, L.; Jin, C.; Li, D.; Liu, J.; Huang, S. Irradiation-Induced Luminescence Enhancement Effect of ZnS:Mn^{2+} Nanoparticles in Polymer Films. *Opt. Lett.* **1997**, *22*, 913–915.
53. Biju, V.; Makita, Y.; Sonoda, A.; Yokoyama, H.; Baba, Y.; Ishikawa, M. Temperature-Sensitive Photoluminescence of CdSe Quantum Dot Clusters. *J. Phys. Chem. B* **2005**, *109*, 13899–13905.
54. Califano, M.; Franceschetti, A.; Zunger, A. Temperature Dependence of Excitonic Radiative Decay in CdSe Quantum Dots: The Role of Surface Hole Traps. *Nano Lett.* **2005**, *5*, 2360–2364.
55. Lubyshev, D. I.; Gonzalez-Borrero, P. P.; Marega, E.; Petitprez, E.; Scala, N. L.; Basmaji, P. Exciton Localization and Temperature Stability in Self-Organized Inas Quantum Dots. *Appl. Phys. Lett.* **1996**, *68*, 205–207.
56. Gerion, D.; Pinaud, F.; Williams, S. C.; Parak, W. J.; Zanchet, D.; Weiss, S.; Alivisatos, A. P. Synthesis and Properties of Biocompatible Water-Soluble Silica-Coated CdSe/ZnS Semiconductor Quantum Dots. *J. Phys. Chem. B* **2001**, *105*, 8861–8871.
57. Parak, W. J.; Gerion, D.; Zanchet, D.; Woerz, A. S.; Pellegrino, T.; Micheel, C.; Williams, S. C.; Seitz, M.; Bruehl, R. E.; Bryant, Z. Conjugation of DNA to Silanized Colloidal Semiconductor Nanocrystalline Quantum Dots. *Chem. Mater.* **2002**, *14*, 2113–2119.
58. Katre, N. V. The Conjugation of Proteins with Polyethylene Glycol and Other Polymers. Altering Properties of Proteins to Enhance Their Therapeutic Potential. *Adv. Drug Delivery Rev.* **1993**, *10*, 91–114.
59. Roberts, M. J.; Bentley, M. D.; Harris, J. M. Chemistry for Peptide and Protein Pegylation. *Adv. Drug Delivery Rev.* **2002**, *54*, 459–476.
60. Jayagopal, A.; Russ, P. K.; Haselton, F. R. Surface Engineering of Quantum Dots for *In Vivo* Vascular Imaging. *Bioconjugate Chem.* **2007**, *18*, 1424–1433.
61. Yu, W. W.; Qu, L.; Guo, W.; Peng, X. Experimental Determination of the Extinction Coefficient of CdTe, CdSe, and CdS Nanocrystals. *Chem. Mater.* **2003**, *15*, 2854–2860.
62. Fischer, H. C.; Fournier-Bidoz, S.; Pang, K. S.; Chan, W. C. W. Quantitative Detection of Engineered Nanoparticles in Tissues and Organs: An Investigation of Efficacy and Linear Dynamic Ranges Using Icp-Aes. *NanoBiotechnology* **2007**, *3*, 46–54.